A Journal of the Gesellschaft Deutscher Chemiker

Angewandte

GDCh

International Edition

Chemie

www.angewandte.org

Accepted Article

Title: Mapping the Excited State Potential Energy Surface of a Photomolecular Motor

Authors: Stephen Roy Meech, Chris Hall, Ben Feringa, and Wesley Browne

To be cited as: *Angew. Chem. Int. Ed.* 10.1002/anie.201802126
Angew. Chem. 10.1002/ange.201802126

Link to VoR: http://dx.doi.org/10.1002/anie.201802126
http://dx.doi.org/10.1002/ange.201802126

WILEY-VCH

10.1002/anie.201802126

Mapping the Excited State Potential Energy Surface of a Photomolecular Motor

Christopher R. Hall[a], Wesley R. Browne[b], Ben L. Feringa[c]* and Stephen R. Meech[a]*

Abstract: A detailed understanding of the operation and efficiency of unidirectional photomolecular rotary motors is essential for their effective exploitation in molecular nanomachines. Unidirectional motion relies on light driven conversion from a stable (**1a**) to a metastable (**1b**) conformation, which then relaxes via a thermally driven helix inversion in the ground state. The excited state surface has thus far only been experimentally characterised for **1a**. Here we probe the metastable, **1b**, excited state, utilising ultrafast Transient Absorption and Femtosecond Stimulated Raman Spectroscopy. These reveal that the 'dark' excited state intermediate between **1a** and **1b** has a different lifetime and structure depending on the initial ground state conformation excited. This suggests that the reaction coordinate connecting **1a** to **1b** differs to that for the reverse photochemical process. The result is contrasted with earlier calculations.

Light driven molecular motors based on the chiral overcrowded alkene motif convert the energy of incident photons into intramolecular rotational motion.[1] As such they have the potential to act as a power source for the molecular machines of the future.[2] The essential operational features of light driven molecular rotary motors are illustrated in Figure 1.[3] The lowest energy ground state conformation (**1a**) comprises a 'stator' linked via a double bonded 'axle' connected to a 'rotor', which has a stereogenic centre. The molecule is nonplanar due to steric strain. Excitation of the lowest energy π to π^* transition localised on the axle reduces the bond order, releasing steric strain and hence a barrierless structural relaxation. The result of this excited state structure change is isomerization leading ultimately to population of the metastable ground state **1b** with a yield of 5 – 20% depending on the substituents.[4] The conformation **1b** can then relax to **1a** by a ground state thermal isomerization either in the reverse or the forward direction, but the forward helix inversion step is overwhelmingly favored due to a lower energy barrier, leading to a half rotation and, for the symmetrical motors studied here, population of **1a** but rotated by 180□ (Figure 1). Absorption of a second photon followed by a second forward helix inversion completes one cycle of rotor motion. Optimization of the molecular structure has led to motors of the general structure **1a** with rotation rates in the MHz frequency range.[3b] Recent synthetic advances demonstrated cooperative rotation of two coupled motors.[5] Although progress has been rapid, many challenges remain before such motors form components of functioning molecular machines, including: more detailed understanding of the structure change accompanying excited state reaction; understanding how structure change couples to molecular environment; knowledge and control of the photochemical quantum yield. Each of these requires an accurate picture of the excited state potential energy surface (PES) and its coupling to the ground state.

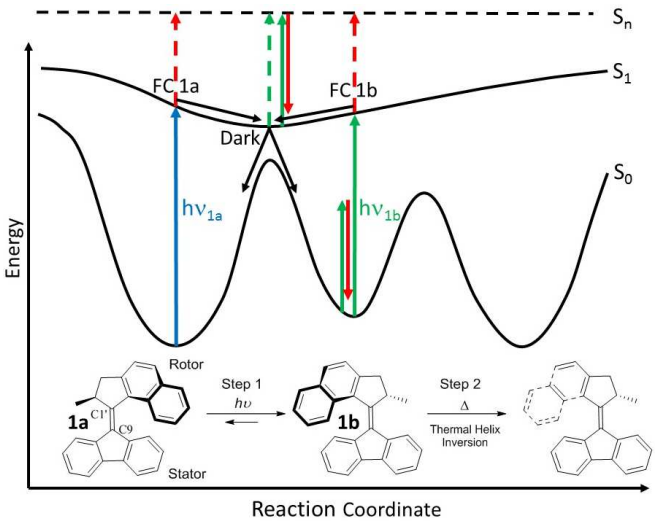

Figure 1. Schematic one dimensional PES for molecular motors. Structure **1a** is the thermodynamically stable molecular motor and **1b** the metastable form generated photochemically from **1a**. The states studied in this work are shown, with colored arrows indicating optical transitions between them. Single solid lines are excitation wavelengths, dashed lines indicate states measured in TA and green/red pairs of lines represent states probed by FSRS. Solid black arrows indicate structural relaxation and internal conversion at conical intersections (not shown).

Previously we characterized the excited state dynamics of **1a** by ultrafast Time-Resolved Fluorescence (TRF), Transient Absorption (TA) and Femtosecond Stimulated Raman Spectroscopy (FSRS).[4, 6] The initial Franck-Condon (FC) excited state was observed to relax in ca 100 fs to a 'dark' (i.e. with negligible transition moment to S_0) state which undergoes fast intramolecular vibrational cooling and picosecond excited state relaxation, leading to formation of a vibrationally hot **1b** ground state. Similar measurements using transient IR spectroscopy were reported in a joint theoretical and experimental study.[7] These studies of **1a** excited state dynamics stimulated high quality quantum chemical calculations.[7-8] Three recent examples point to a reaction coordinate that involves both pyramidalization at the

[a] Dr Christopher R. Hall and Prof. Dr Stephen R. Meech*
Chemistry
University of East Anglia
Norwich NR4 7TJ, UK
E-mail: s.meech@uea.ac.uk
[b] Prof. Dr Wesley R. Browne
Molecular Inorganic Chemistry, Stratingh Institute for Chemistry
University of Groningen
Nijenborgh 4, 9747 AG Groningen, Netherlands
[c] Prof Dr Ben L. Feringa*
Synthetic Organic Chemistry, Stratingh Institute for Chemistry
University of Groningen
Nijenborgh 4, 9747 AG Groningen, Netherlands

Supporting information for this article is given via a link at the end of the document

10.1002/anie.201802126

fluorenyl – axle carbon (C9) and torsional motion about the axle; consistent with the observed solvent friction dependence.[4, 8d, 8f, 8h] These calculations reveal the fundamentally multidimensional nature of the reaction coordinate (in contrast to the 1D Figure 1). Torsion and pyramidalization coordinates comprise a basin-like excited state PES with the dark state minimum around which FC**1a**, FC**1b** and two conical intersections (CIs) are located. Here we probe experimentally the pathway from FC**1b** and contrast it with **1a** excitation. However, the calculations are not entirely self-consistent. Two suggest that dynamics involve a crossing of two excited states, while two others find that the dynamics occur on a single PES.[8d, 8f] Furthermore, two have investigated the entire **1a**/**1b** PES in both ground and excited states, which has not yet been characterized experimentally. Kazaryan et al calculated excited state decay dynamics following both **1a** and **1b** excitation, reporting an overall slower decay for **1b**, while Pang et al made a detailed simulation of excited state dynamics following **1b** excitation, but did not track the pathway for **1a** excitation.[8d, 8f]

Here we present the first detailed experimental study of excited state dynamics following excitation of the metastable **1b** form, and contrast them with data for **1a**. We follow the population dynamics using TA and probe dark state structures with FSRS; transitions and structural dynamics probed are indicated in Figure 1. Remarkable differences are found between **1a** and **1b** excited state structures and dynamics, suggesting distinct relaxation pathways; these data are not in complete agreement with recent calculations, and thus present a future challenge to theory.

Figure 2A shows the measured absorption spectra for **1a** and for the photostationary state (**1a** + **1b**) obtained on continuous irradiation at 385 nm, along with the absorption spectrum of **1b** calculated from them (Supporting Information (SI) S11). The solvent is cyclohexane. As previously described **1b** is red shifted with respect to **1a**.[9] Excitation at 450 nm exclusively pumps the S_0 S_1 transition of **1b**. Figure 2B shows the TA spectrum for **1b** recorded 100 fs after excitation at 450 nm by 100 fs pulses; it is contrasted with the same spectrum for **1a** excited at 405 nm (which matches that reported for 390 nm excitation[6b]). The time dependent TA spectra of **1b** are shown for completeness (Fig. S1). The two TA spectra are similar but there are significant differences. Both show two transitions, the lower energy transition (*ca.* 740 nm) is ascribed to the FC state, which decays rapidly (~100 fs) to an equilibrium between it and a dark state, which absorbs near 520 nm. These two transitions are slightly blue shifted compared to the TA spectra of **1a**. The dark state spectrum formed following **1b** excitation also has a steeper profile on the blue edge than observed for **1a**, which reflects the negative contribution below 500 nm arising from the ground state bleach (the bleach recovery dynamics are shown in Fig. S2). A much more remarkable difference becomes apparent from the comparison of the time dependences (Fig. 2C). The dark state formed on **1a** excitation was previously shown to act as the precursor to formation of the (vibrationally hot) **1b** product with a lifetime of 1.6 ps.[4, 6b] A dark state with a similar spectrum is formed following excitation of **1b** (Fig. 2B), but its decay is markedly accelerated, by a factor of ca 7 (Fig. 2C) compared to that of **1a**.

The observation of an accelerated decay for the dark state populated on **1b** excitation is significant, as it shows again that the one-dimensional potential surface imagined in Fig. 1 is too

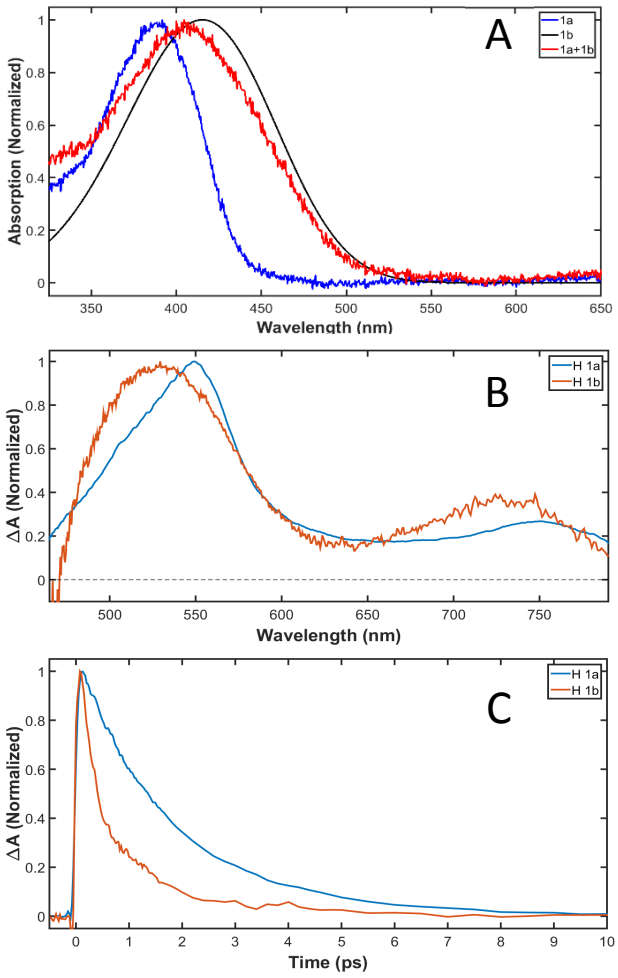

Figure 2. A. Absorption spectra of **1a** (blue), the photostationary state **1a** + **1b** (red) and the calculated **1b** spectrum (black). The excitation wavelengths used for **1a** and **1b** excitation are 405 nm and 450 nm respectively. B. Transient absorption for **1a** (blue) and **1b** (orange) excitation, recorded 100 fs after excitation. C. Population decay for **1a** and **1b** excitation; pulse width 100 fs.

simple – the dark states reached following excitation of **1a** and **1b** are not the same, or at least have significantly different relaxation rates. We note that this finding correlates with the experimental report of a 1:3.5 ratio of forward:reverse quantum yields.[4] Furthermore, the calculations of Kazaryan et al reported a difference in yield following excitation of **1a** and **1b** (albeit for a motor of significantly different structure to that studied here). However, in that case the **1b** excited state was calculated to be longer lived than **1a**, which differs from the present result (Fig. 2C).[8d]

Whether the dark states reached by excitation of the different ground states have different structures as well as decay rates is important, and can in principle be resolved by transient vibrational spectroscopy. We recently showed that FSRS reveals details of the relaxation in **1a** from the FC state to the dark state and onwards to **1b**.[6b] It is thus interesting to compare the structures of the dark states reached by the different excitation routes. Unfortunately the rapid decay which dominates the early

10.1002/anie.201802126

part of the relaxation of the dark state formed from **1b** (Fig. 2C) means that the FSRS would be measured in the region of pulse overlap, which leads to contributions from 'coherent artefacts' which can distort FSRS data. To obtain high quality spectra for the dark state we exploit the earlier observation that the introduction of a cyano substituent at the 5' positon on the naphtyl rotor (**1a-CN**, Fig. S10) results in an extended lifetime for the dark state, arising from a modification to the excited state surface, but yields otherwise similar behavior to **1a**.[4] We repeated the TA measurements for **1a-CN** and **1b-CN**, and recovered qualitatively the same results as for **1a**/**1b**; TA are blue shifted for excitation of **1b-CN**, and the lifetime of the dark state is significantly shortened, in this case from ca 10 ps to 3 ps, with the decay of **1a-CN** being well represented by single exponential kinetics, while the faster **1b-CN** decay departs slightly from single exponential behavior, a result which may reflect incomplete vibrational cooling following the 100 fs FC state decay[4,6b] (Figs. 3A,B; corresponding time dependent TA and fits are shown in Figs. S3-S6).

The longer lifetime of the dark state facilitates time resolved FSRS, and data for **1a-CN** and **1b-CN** are contrasted in Fig. 3C, and shown as a function of time in Fig. 3D. Fig. 3C compares the Raman spectra of dark states reached via **1a-CN** and **1b-CN** (averaged between 200 fs and 500 fs to improve signal-to-noise – the full temporal evolution is shown in Figs. 3D and S7). The FSRS spectra differ in two respects. First, in the higher wavenumber region (>1000 cm^{-1}) the most intense peak is at 1460 cm^{-1} in **1b-CN** but red shifted to 1350 cm^{-1} in **1a-CN**. There are other smaller differences in this region, with the most intense FSRS peak for **1b-CN** being broader than for **1a-CN**. In the lower frequency region there is a second major difference with the mode at 350 cm^{-1} for **1a-CN** absent or strongly shifted for **1b-CN**. These differences point to distinct structures for the two dark states reached from different ground states. Aside from these notable differences there is overlap between the two FSRS, with many modes showing the same or similar frequencies and amplitudes (as expected, since they are localized on the two aromatic rings and therefore less likely to be involved in the reaction coordinate and thus modified on dark state formation[6b]).

Although the observed differences in FSRS point to distinct structures, the assignment of the spectral changes is less straightforward. This is partly because the calculations which aided assignment of ground state vibrational modes[6b] are less readily obtained for excited electronic states of large molecules on reactive potential surfaces. For **1a** the FSRS data were discussed earlier.[6b] In the ground state there are a few intense Raman active modes mainly involving C=C stretches of the 'axle'. The excited state spectrum is much more complex, and overall shifted to lower wavenumber. The shift to lower wavenumber can be assigned to a reduced bond order on the 'axle'. The increased complexity was previously ascribed to the different resonances (S_0 S_1 and S_1 S_n) on which the spectra are generated, leading to different enhancement patterns.[6b] These arguments apply to **1b-CN**, where increased complexity and an overall red shift compared to the ground state are also observed (Figs. S7,8). It is the complexity of the S_1 spectra that prohibits a direct assignment of the blue shift observed between **1a-CN** and **1b-CN** (Figure 3C) to a specific structural change, for example, to a shortening of the 'axle' C=C bond in the **1b-CN** dark state; this could be investigated through quantum chemical calculations.

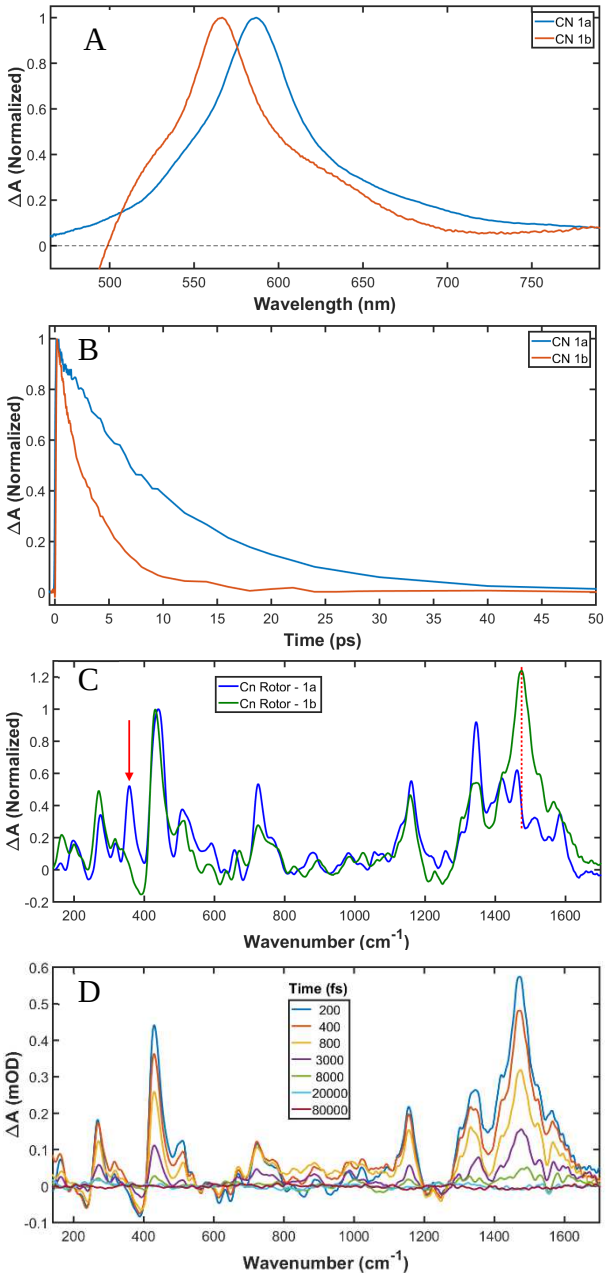

Figure 3. A. The TA spectra for **1a-CN** (blue) and **1b-CN** (orange). B. The decay kinetics of the dark state for **1a-CN** (blue) and **1b-CN** (orange). C. The FSRS recorded for **1a-CN** and **1b-CN** measured between 200 and 700 fs (averaged). D Time resolved FSRS for **1b-CN** excitation.

A second potential contribution to the spectral changes in Fig. 3C is different resonance conditions for **1a-CN** and **1b-CN**. It has been shown experimentally and in theory that FSRS spectra may depend on the resonance wavelength.[10] To check for this we recorded FSRS for **1a-CN** at wavelengths across the transient spectrum. At least on the Stokes side of the S_1 S_n dark state transition (where all present FSRS measurements were made) the spectra are only a weak function of Raman wavelength, and do not reproduce the changes observed between **1a-CN** and **1b-CN** (Fig. S9). Thus, the structure change between dark states

detected in FSRS is real, although, in the absence of accurate excited state calculations of vibrational spectra, structural assignment is elusive.

The time dependence (Fig. 3D) shows no temporal evolution in the FSRS spectrum of **1b-CN** dark state during its lifetime, suggesting that thermalization of the vibrationally hot dark state formed in 100 fs from the FC state is essentially complete on the timescale of its 3 ps lifetime, consistent with the near exponential decay observed (Fig. S6). Note that the hot ground state formed as the dark state decays is detected at ca 1560 cm^{-1} and itself decays in tens of picoseconds as the ground state cools. This is as observed for **1a**[6b] but for both **1a-CN** and **1b-CN** the ground state signal is much weaker, as the Raman pump wavelength is further from resonance with the S_0 absorption.

The present results establish that excitation of the metastable **1b** molecular motor is followed by ultrafast decay of the FC state to a dark state with a markedly reduced lifetime and distinct structure, compared to that accessed from the thermodynamically favored **1a** state. Thus, either the dark state reached following **1a** or **1b** excitation is not common to the two ground states, or the way in which it is prepared results in the different lifetimes observed, for example by accessing different CIs for internal conversion to the ground state. These results can be discussed in the context of the two calculations which included the **1b** excited state surface. Pang et al found that the S_1 surface had a single minimum, independent of the initial geometry.[8f] If that were the case then the observed difference in lifetime for that common state must reflect dynamical effects, i.e. the pathway from the different initial geometries, rather than the final state reached. This is conceivable for **1a/b**, as the initial decay of the dark state reached via **1b** is very fast (ca 200 fs, Fig. 2C) and may not be thermalized during its lifetime. However, the lifetime for **1b-CN** is 3 ps, which is adequate for thermalization, so the different decay times observed suggests distinct minima. Different minima in-turn suggests different structures, consistent with the vibrational spectra observed (Fig. 3C). Kazaryan et al. presented calculations for a somewhat different motor to that studied here (and by Pang et al), and found distinct minima on S_1 associated with the **1a** and **1b** states; this is consistent with the present observations.[8d] However, the lifetimes on the excited state surface were calculated to be slightly longer for the **1b** than the **1a**-like form, which is the opposite to our observations (albeit for a different molecule) (Figs. 2C, 3B). The dark state decay time will depend sensitively on the relative locations and energies of the minima and CIs with the ground states, so high level quantum mechanical calculations will be required to reproduce the present data, and even then medium effects might introduce significant differences. These result further suggest that the different motor structures may exhibit significant differences in excited state dynamics; further work is in progress on this.

In summary, excited state structure and dynamics for the metastable state of a molecular rotor have been measured for the first time, and contrasted with data for the stable form. Both states decay to intermediate dark states on an ultrafast (ca 100 fs) timescale, but the dark states attained have distinct structures and lifetimes. Neither feature was predicted by calculations. Thus, these data should stimulate further theoretical investigations of excited state dynamics which, together with further experiments, will provide an accurate and detailed view of the excited state potentials of molecular rotors.

Experimental Section

The methods and conditions for TA, FSRS and data analysis are described in detail SI 12 and elsewhere.[6b] The FSRS data were measured as Raman gain on the low energy side of the Raman pump wavelength. The synthesis and characterization of **1a** and **1a-CN** were presented previously.[9]

Acknowledgements

SRM is grateful to EPSRC for financial support (EP/J009148/01, EP/M00197/1). BLF gratefully acknowledge generous support from NanoNed, The Netherlands Organization for Scientific Research (NWO-CW Top grant to BLF), the Royal Netherlands Academy of Arts and Sciences (KNAW), the Ministry of Education, Culture and Science (Gravitation program 024.001.035) and the European Research Council (Advanced Investigator Grant No. 694345 to BLF).

Keywords: Ultrafast • Molecular Motor • Photochemistry • Excited State • Dynamics

[1] aW. Szymanski, J. M. Beierle, H. A. V. Kistemaker, W. A. Velema, B. L. Feringa, *Chem. Rev.* **2013**, *113*, 6114-6178; bB. L. Feringa, *Acc. Chem. Res.* **2001**, *34*, 504-513; cB. L. Feringa, *J. Org. Chem.***2007**, *72*, 6635-6652.

[2] aV. Balzani, A. Credi, M. Venturi, *Chem.Soc. Revi.***2009**, *38*, 1542-1550; bE.R. Kay and D.A. Leigh Angew. Chem. Int. Ed. **2015**, *54*, 10080-10088; cW.R.Browne and B.L. Feringa Nat. Nanotecnol. **2006**, *1*, 25-35; dJ.P. Sauvage and P. Gaspard, (**2010**) From Non-covalent Assemblies to Molecular Machines (Wiley-VCH); eC.J. Burns and J. Fraser Stoddart (**2016**) The Nature of the Mechanical Bond: From Molecules to Machines (J. Wiley and Sons); fK. Kinbara and T Aida Chem. Rev. **2005**, *105*, 1377-1400.

[3] aM. Klok, L. Janssen, W. R. Browne, B. L. Feringa, *Faraday Disc.* **2009**, *143*, 319-334; bJ. Vicario, A. Meetsma, B. L. Feringa, *Chem.Comm.***2005**, 5910-5912.

[4] J. Conyard, A. Cnossen, W. R. Browne, B. L. Feringa, S. R. Meech, *J. Amer. Chem. Soc.* **2014**, *136*, 9692-9700.

[5] J. C. M. Kistemaker, P. Stacko, J. Visser, B. L. Feringa, *Nat. Chem.* **2015**, *7*, 890-896.

[6] aJ. Conyard, K. Addison, I. A. Heisler, A. Cnossen, W. R. Browne, B. L. Feringa, S. R. Meech, *Nat. Chem.* **2012**, *4*, 547-551; bC. R. Hall, J. Conyard, I. A. Heisler, G. Jones, J. Frost, W. R. Browne, B. L. Feringa, S. R. Meech, *J. Amer. Chem. Soc.* **2017**, *139*, 7408-7414.

[7] S. Amirjalayer, A. Cnossen, W. R. Browne, B. L. Feringa, W. J. Buma, S. Woutersen, *J.Phys. Chem. A* **2016**, *120*, 8606-8612.

[8] aA. Nikiforov, J. A. Gamez, W. Thiel, M. Filatov, *J.Phys. Chem. Letts* **2016**, *7*, 105-110; bM. Filatov, M. Olivucci, *J J. Org. Chem* **2014**, *79*, 3587-3600; cY. Amatatsu, *J. Phys. Chem. A* **2013**, *117*, 12529-12539; dA. Kazaryan, Z. Lan, L. V. Schafer, W. Thiel, M. Filatov, *J.Chem.Theory and Comp.* **2011**, *7*, 2189-2199; eA. Kazaryan, J. C. M. Kistemaker, L. V. Schafer, W. R. Browne, B. L. Feringa, M. Filatov, *J. Phys. Chem. A* **2010**, *114*, 5058-5067; fX. Pang, X. Cui, D. Hu, C. Jiang, D. Zhao, Z. Lan, F. Li, *J. Phys. Chem. A* **2017**, *121*, 1240-1249; gF. Liu, K. Morokuma, *J. Amer.*

10.1002/anie.201802126

Chem. Soc. **2012**, *134*, 4864-4876; hY. Y. Li, F. Y. Liu, B. Wang, Q. Q. Su, W. L. Wang, K. Morokuma, *J.Chem. Phys.***2016**, *145*.

[9] M. M. Pollard, P. V. Wesenhagen, D. Pijper, B. L. Feringa, *Org. Biomolec.Chem.***2008**, *6*, 1605-1612.

[10] aS. Umapathy, B. Mallick, A. Lakshmanna, *Journal of Chemical Physics* **2010**, *133*; bB. G. Oscar, C. Chen, W. M. Liu, L. D. Zhu, C. Fang, *J. Phy. Chem A* **2017**, *121*, 5428-5441; cS. Kayal, K. Roy, S. Umapathy, *J.Chem. Phys.***2018**, *148*.

10.1002/anie.201802126

WILEY-VCH

Entry for the Table of Contents (Please choose one layout)

Layout 1:

COMMUNICATION

Starting motors. Excited state structure and dynamics in a light driven unidirectional motor are shown to be a function of the initial excitation geometry.

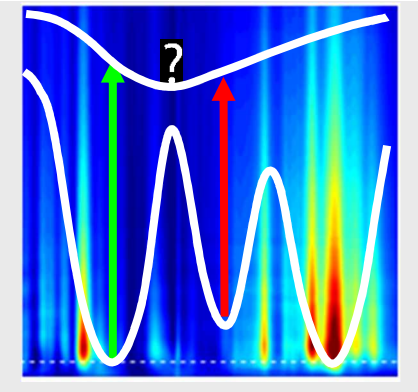

Christopher R. Hall, Wesley R. Browne, Ben L. Feringa and Stephen R. Meech**

Page No. – Page No.

Mapping the Excited State Potential Energy Surface of a Photomolecular Motor